

1 **Supplementary Information**

2

3 **Supplementary Methods**

4 *Site selection and sampling*

5 Samples were collected from two sites during an oceanographic voyage (IV2015_V03) in the East
6 Australia Current (EAC) region in austral winter (June 2015) aboard the *R/V Investigator*,
7 Australia's Marine National Facility managed by CSIRO. Vertical profiles of temperature (SBE3T
8 S/N, Sea-Bird Scientific, USA), salinity (measured as conductivity SBE4C S/N, Sea-Bird
9 Scientific, USA), dissolved oxygen (SBE43 S/N, Sea-Bird Scientific, USA) and chlorophyll-*a*
10 fluorescence (Aquatrack III, Chelsea Technologies Group, UK), were measured using a CTD
11 (conductivity-temperature-depth)-profiler. Sensors were calibrated by on-board analyses using a
12 Guildline Autosal Laboratory Salinometer 8400(B) – SN 71611, and an automated Photometric
13 Oxygen system (Scripps Institute of Oceanography). Mixed layer depth (MLD) was calculated as
14 the depth where potential density is $+0.125 \text{ kg m}^{-3}$ relative to the surface using the `get_mld` Matlab
15 function. Absolute temperature was converted to potential temperature using the CSIRO SeaWater
16 library function 'sw_ptmp' and this was then used to calculate potential density 'sw_dens.'

17

18 Dissolved nutrients (phosphate, silicate, nitrite, nitrate and ammonium) were analysed from Niskin
19 bottle samples. A segmented flow auto-analyser Seal AA3HR was used, following the standard
20 operational procedures (SOP 001-004) modified from published methods by the CSIRO Oceans
21 and Atmosphere Hydrochemistry Team to optimise nutrient analysis at sea. Briefly, phosphate was
22 determined using the molybdenum blue method, based on Murphy and Riley (1962) with
23 modifications from the NIOZ-SGNOS Practical Workshop (2012). Silicate was also measured
24 using the molybdenum blue method, and nitrite and nitrate using the Copper-cadmium reduction

25 – Naphthylenediamine photometric method, both based on Armstrong et al (1967). Ammonium
26 was analysed using the ortho-phthaldialdehyde method based on K  rouel and Aminot 1997. The
27 accuracy of nutrient analysis was determined by analysing a certified reference material produced
28 by KANSO, Japan. The RMNS Lot CA (produced 22/02/2013) was measured four times in every
29 analytical run. The RMNS Lot CD (produced 08/04/2015) was analysed twice alongside the CA
30 Lot. RMNS results were converted from $\mu\text{mol}/\text{kg}$ to $\mu\text{mol L}^{-1}$ at 21  C.

31

32 Seawater containing microbial communities was collected in 12 L Niskin bottles using a 24 bottle
33 CTD-rosette sampler. From there, samples were gently dispensed via silicon tubing into plastic
34 containers before being aliquoted into replicate borosilicate flat-bottomed glass vials (30 mL
35 capacity). Tubing and all vessels were acid-washed to minimize metal contamination. Vials
36 containing seawater aliquots were then randomly allocated to temperature treatments within a
37 thermal gradient block.

38

39 *Experimental set up*

40 Microbial communities were incubated within 2 h of collection under $\sim 75 \mu\text{mol photons m}^{-2} \text{ s}^{-1}$
41 (below the photosynthesis saturation irradiance (Bouman et al. 2017) so as not to induce additional
42 ROS production from high light stress, but likely not representative of the dynamic light conditions
43 in the mixed layer), maintained using LED light panels (Cidley, China). Illumination was set to a
44 12:12 light dark cycle to reflect the average natural diurnal cycle. The experimental design entailed
45 exposing microbial communities to a range of temperatures spanning 7   C below and 10   C above
46 ambient temperature (~ 22   C for both sites) using a thermal gradient block. The thermal block was
47 made of solid aluminium machined to form replicate wells to house flat-bottom vials, with the

48 temperature gradient created by pumping cold water into one end and hot water into the other
49 (resulting in a temperature range from 15.6 to 32.1 °C). This design was intended to test the acute,
50 not acclimated, response to temperature as a way of gaining insight into the thermal performance
51 of populations that may diverge due to previous thermal exposure. Microbes were placed into
52 experimental treatments where temperature would have equilibrated within 0.5 h. For comparison,
53 thermal trajectories extracted from a global circulation model using Lagrangian tracking software
54 (Doblin and van Sebille, 2016), show the maximum change in microbial temperature exposure is
55 approximately 5 °C over a 5-d period (i.e., 1 °C per day).

56

57 *Physiological response to short-term temperature excursions*

58 To understand the physiological responses of microbes to temperature changes, we quantified their
59 intracellular reactive oxygen species (ROS) content at 4 time points: at the beginning of the
60 experiment (local time ~10:00, ~4 h after sunrise) and 1, 5, and 25 h later (i.e., T0, T1, T5, T25 h,
61 respectively). This allowed ROS to be measured during the natural light period. Commercially
62 available fluorescent markers for superoxide (488 nm blue excitation; 580 nm orange emission)
63 and other ROS (488 nm blue excitation; 530 nm green emission) (Total ROS/Superoxide detection
64 kit ENZ-51010, Enzo Life Sciences, Inc., New York, USA) were used within their 6-month shelf
65 life. Prior to the voyage, the protocol was optimised for use with phytoplankton, whereby a matrix
66 of fluorescent dye incubation time and concentration for both dyes was tested. Optimal staining
67 conditions were achieved at 1:1000 for superoxide stain (orange) and 1:2000 for other ROS stain
68 (green) both incubated in the dark at the experimental temperature for 1 h before flow cytometric
69 analysis. Initial samples for positive (induced using kit) and negative (no stain) controls were
70 aliquoted and run on board (confirming stain optimisation for the different samples) using an

71 Influx flow cytometer (BD Biosciences). T0 samples were also analyzed to measure ambient
72 background ROS within each population (Fig. S2).

73

74 During the experiment, subsamples were removed from glass vials and placed into tubes, stain
75 added, and tubes incubated in the dark for 1 h under incubation conditions. Following incubation,
76 a 10 μ l aliquot of standard 1.0 μ m yellow-green fluorescent beads was added (Fluoresbrite® YG
77 Microspheres 1.00 μ m (Cat#17154-10); Polysciences Inc., Taipei, Taiwan) to tubes and stained
78 samples interrogated using a flow cytometer (BD Influx, Becton Dickson, Brussels, Belgium)
79 equipped with a 50 mW blue laser emitting at a fixed wavelength of 488 nm. Picoplankton
80 populations were discriminated as low phycoerythrin (PE-580/30 nm) high chlorophyll-*a* (Chl-
81 692/20 nm) cells and gated according to Fig. S1A.

82

83 Gated picoeukaryotes were then investigated for their ROS content using “daughter” biplots of
84 green (530 ± 20 nm; 530/40 nm) vs orange (530 ± 15 nm; 580/30 nm) fluorescence (Fig. S1;
85 FlowJo, LLC, Ashland Oregon). To estimate ROS accumulation, unstained T0 populations were
86 used to define ‘healthy’ cells so that ROS expression would be quantified as an increase from
87 background (Fig. S2). The stained samples were then used to determine ROS content of cells under
88 incubation conditions; a gate depicting ‘stressed’ cells was made using boolean logic (Fig. S1).

89

90 The median forward scatter and fluorescence (580, 530 nm) were extracted for standard beads and
91 ‘healthy’ and ‘stressed’ cells in all samples. To quantify changes in the relative fluorescence of
92 ‘stressed’ cells over time, scatter and fluorescence values were normalized to forward scatter
93 (FSC) and fluorescence of the standard bead using Equation 1:

94

95 Equation 1: ROS fluorescence (RFU) = ((pico-eukaryote median pop fluor 580* nm/median bead
96 fluor 580* nm)/(pico-eukaryote median pop FSC/median bead FSC))

97 * same equation for 530 nm

98 To assess temperature-induced stress within water masses, normalised fluorescence values for
99 each sample were summed (yielding 530 + 580 fluorescence; Fig. 1A and C) and analysed using
100 ANOVA. T0 values were subtracted from all subsequent time points in order to determine change
101 from the initial condition. We note that PE-containing eukaryotes may change their orange
102 fluorescence with temperature via phycoerythrin pigment content (Chaloub et al. 2015) or through
103 potential changes in the association of phycobilisomes with the thylakoid membrane (Li et al.
104 2001). In this study, we define the pico-eukaryote population as relatively low PE and relatively
105 high Chl-*a* (Fig. S1). As such the relative changes in PE quantified during our ship-board assays
106 should be due to relative changes in ROS content, however care should be taken when applying
107 this method to other studies.

108

109 *Microbial diversity determination*

110 To characterise the diversity of initial microbial communities used in experiments, sampled
111 seawater (4 L) was filtered immediately (within 1 h of arriving on deck) through 0.22 µm Durapore
112 filters (Merck Millipore, Bayswater, VIC, Australia). Filters were folded, placed in cryovials, snap
113 frozen in liquid nitrogen, and stored at -80 °C (<3 months). DNA was extracted using the MoBio
114 PowerWater DNA isolation kit (MoBio Laboratories, Carlsbad, CA, USA) with the following
115 modifications to the manufacturer's instructions. After the addition of PW1, filters were incubated
116 for 10 min at 60 °C. Following Step 10, 650 µL phenol:chloroform:isoamyl alcohol (25:24:1, pH

117 8, Sigma-Aldrich, Castle Hill, NSW, Australia) was added to the sample, vortexed to mix, and
118 centrifuged for 5 min at room temperature. The aqueous phase containing the sample was
119 transferred to a sterile microcentrifuge tube, and the previous step was repeated using 650 μ L
120 chloroform:isoamyl alcohol (24:1, Sigma-Aldrich). The aqueous phase was again transferred to a
121 fresh sterile microcentrifuge tube and the manufacturer's protocol was resumed from Step 15.
122 DNA concentration and purity was measured using a NanoDrop 2000 spectrophotometer (Thermo
123 Fisher Scientific, Waltham, MA, USA) and DNA was stored at -20 °C. 16S rRNA amplicon
124 sequencing was performed on the variable regions V1-V3 using the primer pair 27F (Lane 1991)
125 and 519R (Turner et al. 1999) on an Illumina MiSeq (Illumina, San Diego, CA, USA; Molecular
126 Research LP, Shallowater, TX, USA). 16S rRNA gene sequencing reads were analysed using the
127 QIIME pipeline (Caporaso et al. 2010; Kuczynski et al. 2012). Briefly, paired-end DNA sequences
128 were joined, *de novo* OTUs were defined at 97% sequence identity using UCLUST (Edgar 2010)
129 and taxonomy was assigned against the SILVA database (version 128) using the BLAST
130 algorithm. To estimate the diversity of microbial phototrophs enumerated in experiments,
131 chloroplast OTUs were then filtered out to a separate file and taxonomy was assigned against
132 PhytoREF (Decelle et al. 2015) in QIIME (Caporaso et al. 2010). Chimeric sequences were
133 detected using usearch61 (Edgar 2010) and filtered from the dataset. Sequences were aligned,
134 filtered and alpha diversity parameters were calculated in Primer v6.1 (Clarke & Gorley 2006).
135 OTUs were subsequently grouped at the genus level, and the contribution of specific taxa to each
136 water mass was calculated using the SIMPER routine (Primer v6.1; Clarke & Gorley 2006).

137

138 *Assessment of relationship between temperature and population variables*

139 Relationships between % cells remaining and temperature after 1, 5, and 25 h of exposure were
140 analysed using Generalized Additive Models (GAMs). Specifically, independently at each time
141 point, we allowed for a smoothed effect of temperature on % survival, varying around a parametric
142 mean. Our initial k for determining the dimension of the smoothed effect was 4. Models were fit
143 separately for the EAC and Tasman Sea, using the `gam()` function from the `mgcv` package in R
144 (Wood 2006, 2011). An identical approach was used to analyse the relationship between ROS
145 production and temperature over all three time points. Finally, to consider the relationship between
146 % cells remaining and ROS production, we used a GAM with an additional random effect to
147 capture variation among temperature treatments, employing the `gamm()` function. Prior to analysis,
148 we averaged replicate survival and fluorescence values within time and temperature levels. We
149 elected to treat temperature as a random effect rather than a fixed effect because: (i) we wished to
150 avoid overfitting a relatively limited data set ($n = 36$), and (ii) we considered the explicit effects
151 of temperature in the preceding analyses.

152

153 *Trajectory analysis*

154 A real-time ocean circulation model was used to determine the source of water sampled at both
155 sites and estimate the thermal exposure of entrained microbes in the weeks before sampling. A
156 total of 100 virtual particles were released at the surface at each of the two sites, and then tracked
157 backwards in time with the `Parcels` tool (Lange and Van Sebille, 2017) by integrating the surface
158 velocity fields of the HYCOM + NCODA Global $1/12^\circ$ Analysis (Bleck, 2002). This HYCOM
159 dataset assimilates observational data from satellites, Argo floats and other instruments, and is
160 designed to be as similar to the real ocean flow as possible.

161 In order to establish the thermal history of the samples, the virtual particles were tracked backward
162 in time for 85 days, storing positions and *in-situ* temperatures every day. Subgrid scale diffusion
163 is represented by a Brownian random walk process, with a diffusivity constant of $K = 100 \text{ m}^2\text{s}^{-1}$.
164 ¹. In order to test the sensitivity of the tracking results to the date of sampling, a sensitivity analysis
165 was performed where similar virtual particle experiments were done where the starting dates were
166 moved up to four weeks earlier and later. These data are shown in Fig. S5. All code used in the
167 particle tracking and creation of the plots can be downloaded
168 from https://github.com/OceanParcels/Microbes_EAC.

169

170

171

172 **Supplementary Tables**

173 **Table S1:** Surface seawater properties at the time of sampling and descriptive thermal history
 174 parameters for water and resident organisms arriving to the sampling sites.

	EAC	Tasman Sea
Oceanographic conditions at sampling sites		
Latitude (°S)	30.621	32.788
Longitude (°E)	153.371	153.785
Bottom depth (m)	504	4798
Temperature °C	22.29	21.48
Salinity	35.65	35.68
Dissolved Oxygen (mmol L ⁻¹)	218.92	220.29
Mixed Layer Depth (m)	50	100
NO ₃ (μmol L ⁻¹)	0.19	0.34
PO ₄ (μmol L ⁻¹)	0.08	0.09
Eukaryote community attributes		
Picoeukaryote (cells ml ⁻¹)	4372 ± 200	5985 ± 1221
# OTUs (97%)	151	242
Shannon's Diversity	4.011	4.037
Pielou's Evenness	0.800	0.735
Margalef's Richness	24.192	40.197
Thermal History within real-time ocean (previous 85 days)		
Mean (± SD) temperature °C of trajectories (n = 100)	24.35 ± 1.26	22.68 ± 0.97

175

176

177 **Table S2: Generalised Additive Mixed Model summary for analysis of % cells remaining**
 178 **in EAC.** Overall, the model fitted 81% of the variance in cell survival across temperatures and
 179 time points. Intercept (1 h) is the average % cells remaining across temperatures at T1, one hour
 180 after the incubation started. Change by 5 h/25 h is how much the average % cells remaining has
 181 declined (relative to the value at 1 h) at T5/T25 (5 or 25 h after the incubation started). Smoothed
 182 effect of temperature is the deviation in % cells remaining across temperatures (relative to the
 183 mean % remaining at 1 hr) using a smooth function. A non-significant p value indicates that the
 184 trend with temperature is not significantly different from a flat line (with no slope). Therefore, at
 185 1 h, temperature does not explain additional variation in % cells remaining. The estimated df
 186 values describe the shape of the relationship between %cells remaining and temperature– a value
 187 of 1 suggests that the relationship is linear; a value of 2 suggests that the relationship is
 188 quadratic. Significant p values indicate that the variation in % cells remaining (after accounting
 189 for the mean value) relates to temperature.
 190

Adjusted R2	Deviance explained	GCV	Scale estimate	n
0.779	81%	168.23	142.39	53
Parametric terms				
Estimate	Std. Error	t-value	p-value	
Intercept (1 h)	86.47	2.82	30.7	< 0.001
Change by 5 h	-10.20	3.98	-2.56	0.0138
Change by 25 h	-48.92	4.04	-12.1	< 0.001
Smoothed effect of temperature				
Estimated df	Reference df	F-value	p-value	
At 1 h	2.28	2.63	0.834	0.332
At 5 h	1.00	1.00	9.524	0.003
At 25 h	1.86	2.23	5.970	0.004

191

192

193 **Table S3: Generalised Additive Mixed Model summary for analysis of % cells remaining**
 194 **in Tasman Sea.** Legend as for Table S2. The non-significant p value for change by 5 h indicates
 195 that the average % cells remaining in the Tasman Sea after 5 h is not different from the value at 1
 196 h. However, at 5 h, there is now a significant relationship between % cells remaining and
 197 temperature.
 198

Adjusted R2	Deviance explained	GCV	Scale estimate	n
0.71	75%	228.22	192.84	53
Parametric terms				
	Estimate	Std. Error	t-value	p-value
Intercept (1 h)	98.61	3.27	30.1	< 0.001
Change by 5 h	-3.38	4.63	-0.73	0.469
Change by 25 h	-36.00	4.71	-7.65	< 0.001
Smoothed effect of temperature				
	Estimated df	Reference df	F-value	p-value
At 1 h	1.05	1.11	0.372	0.601
At 5 h	1.76	2.11	11.55	< 0.001
At 25 h	2.40	2.74	15.43	< 0.001

199

200 **Table S4: Generalised Additive Mixed Model summary for analysis of changes in ROS**
 201 **production: 530+580 fluorescence (RFU) in the EAC.** Legend as for Table S2.

202

Adjusted R2	Deviance explained	GCV	Scale estimate	n
0.85	87.4%	8.21e-5	6.83e-5	53
Parametric terms				
	Estimate	Std. Error	t-value	p-value
Intercept (1 h)	0.076	0.0020	38.88	< 0.001
Change by 5 h	-0.031	0.0028	-11.26	< 0.001
Change by 25 h	-0.045	0.0028	-16.17	< 0.001
Smoothed effect of temperature				
	Estimated df	Reference df	F-value	p-value
At 1 h	1.70	2.05	1.17	0.304
At 5 h	2.13	2.49	5.01	0.006
At 25 h	2.00	2.37	2.95	0.046

203

204

205

206

207 **Table S5: Generalised Additive Mixed Model summary for analysis of changes in ROS**
 208 **production: 530+580 fluorescence (RFU) in the Tasman Sea.** Legend as for Table S2.

209

Adjusted R2	Deviance explained	GCV	Scale estimate	n
0.893	90.7%	2.10e-4	1.79e-4	53
Parametric terms				
	Estimate	Std. Error	t-value	p-value
Intercept (1 h)	0.111	0.0032	35.14	< 0.001
Change by 5 h	-0.066	0.0045	-14.78	< 0.001
Change by 25 h	-0.082	0.0045	-18.18	< 0.001
Smoothed effect of temperature				
	Estimated df	Reference df	F-value	p-value
At 1 h	2.34	2.68	19.855	< 0.001
At 5 h	1.46	1.76	0.292	0.681
At 25 h	1.00	1.00	0.083	0.775

210

211

212

213 **Table S6: Generalised Additive Mixed Model summary for analysis of the relationship**
 214 **between % survival and ROS production in the EAC and Tasman Sea.** Intercept represents
 215 the average % survival of pico-eukaryotes from the EAC population across time points and
 216 temperatures. The difference between the average % survival in the Tasman Sea and EAC is
 217 represented by (Tasman Sea – EAC). The smoothed effect of 530+580 fluorescence shows that
 218 % cells remaining declines with ROS fluorescence; in the EAC it declines approximately
 219 linearly, but in the Tasman Sea the relationship is more curvilinear. The random effect represents
 220 the portion of variation in % survival that is attributed to a random effect of temperature.

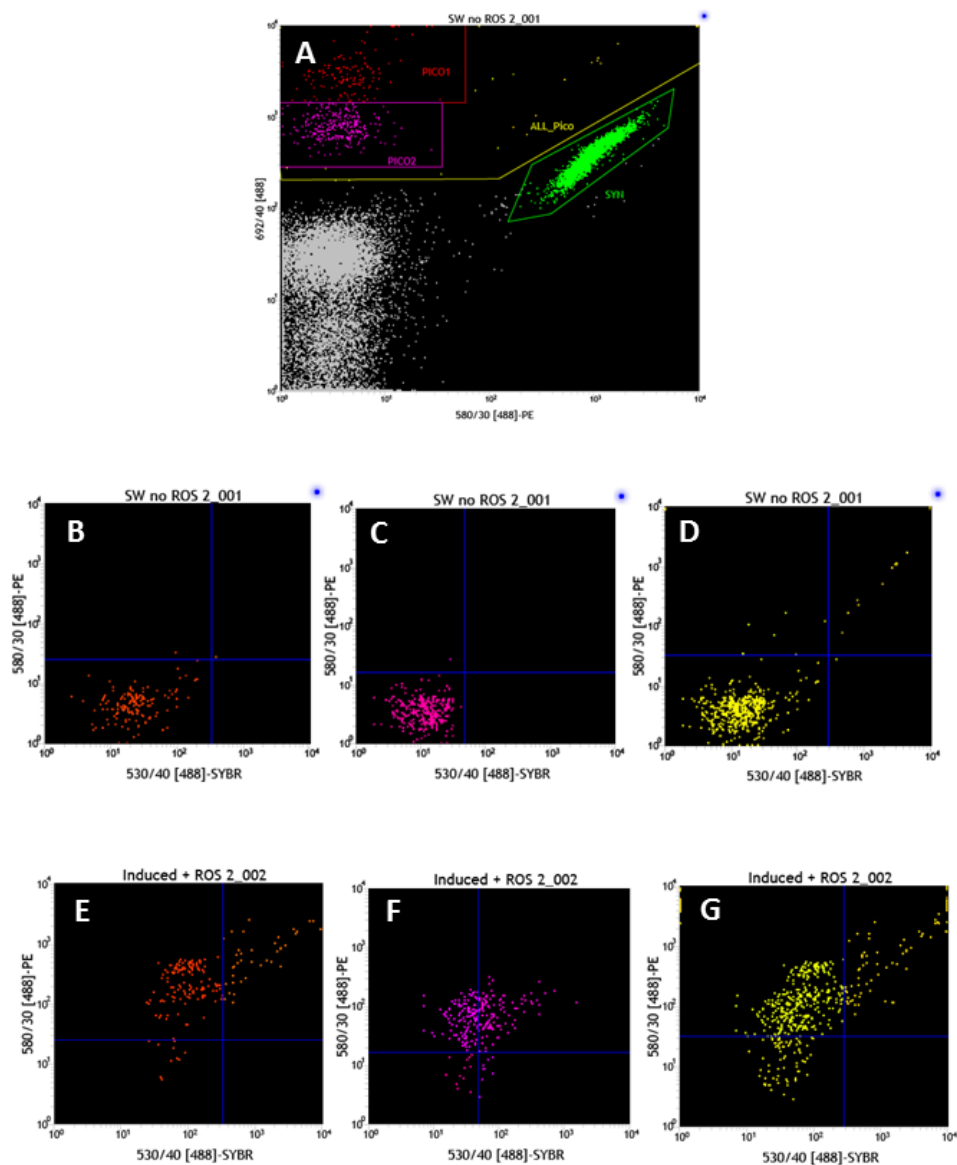
221

Adjusted R²	Scale estimate	n		
0.358	328.08	36		
Parametric terms				
	Estimate	Std. Error	t-value	p-value
Intercept (EAC)	71.55	5.68	12.61	< 0.001
(Tasman Sea – EAC)	12.04	6.39	1.88	0.069
Smoothed effect of 530+580 fluorescence				
	Estimated df	Reference df	F-value	p-value
EAC	1.00	1.00	15.56	< 0.001
Tasman Sea	1.21	1.21	5.56	0.030
Random effect				
	Std. deviation			
Temperature	8.004			

222

223

224

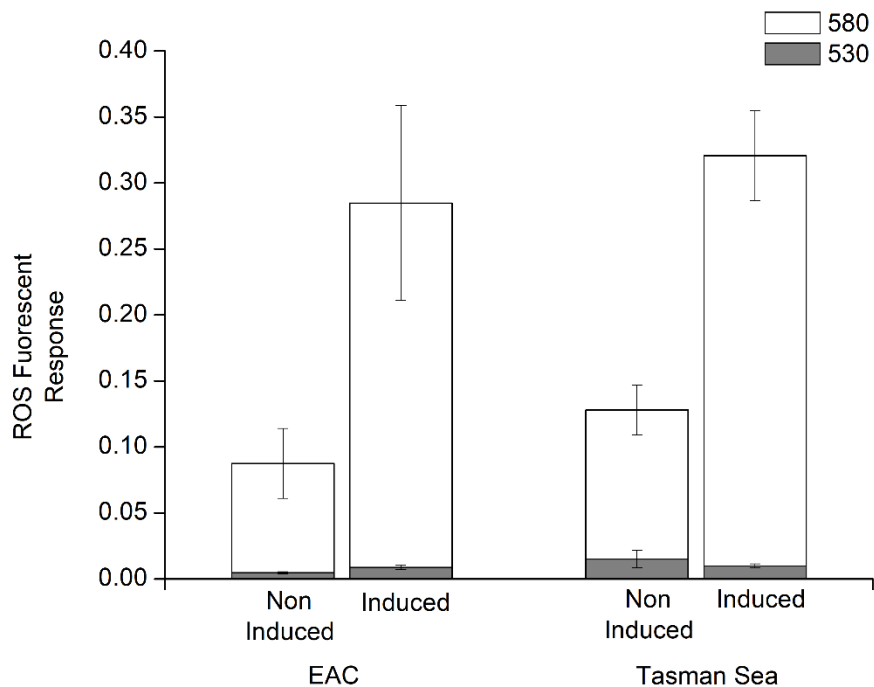


226

227 **Fig S1. Gating logic for flow cytometric analysis of pico-eukaryote populations and ROS**
 228 **production.** Pico-eukaryotes were discriminated from other phototrophs by their relatively low
 229 phycoerythrin and relatively high chlorophyll-*a* content (A). These target cells were divided into
 230 two populations (Pico1 and Pico2) based on chlorophyll-*a* fluorescence, but analyses presented in
 231 the text use the combined Pico1 and 2 population. Cells without any ROS stain (B-D) are shown,
 232 separated into Pico1 (B) Pico2 (C) and all Pico (D). Gates were set on these populations to account
 233 for any autofluorescence in these channels. Positive controls, where cells were induced to produce
 234 ROS are shown in the lower panel, including Pico1 (E), Pico2 (F), all Pico (G), with a positive
 235 shift in orange (580/30 nm) fluorescence indicative of superoxide, and a positive shift in green
 236 (530/30 nm) indicative of all ROS except superoxide.

237

238



239

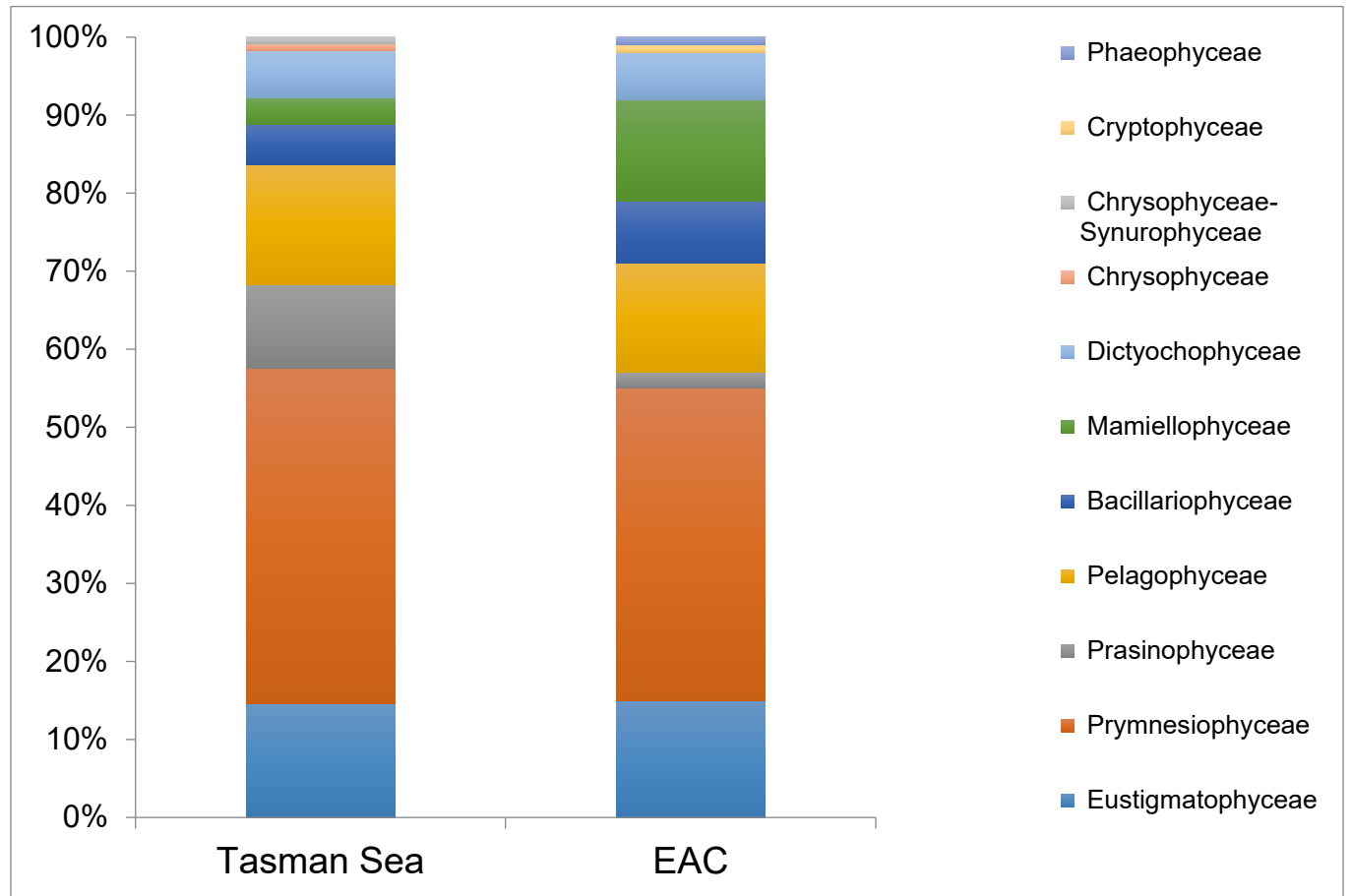
240 **Fig S2. Experimental controls showing initial background ROS in sampled picoeukaryote**
241 **populations versus induced ROS staining.** The commercial kit contains an “induction solution”
242 that causes cells to produce large amounts of ROS (positive control). The non-induced sample
243 (negative control) indicates that there is some ROS already present in the population before they
244 were used in experiments. This base level ROS was both expected and accounted for in our time-
245 course analyses. Plot shows the median fluorescence (normalised to standard fluorescent
246 microspheres) of EAC and Tasman Sea picoeukaryote populations; 580 nm (white) and 530 nm
247 (grey).

248

249

250

251



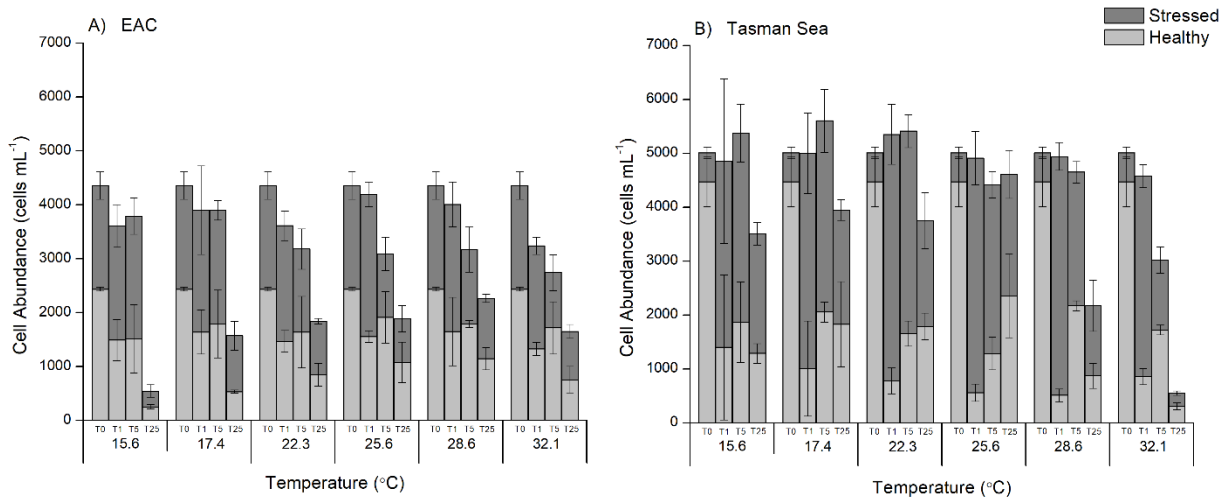
253

254 **Fig S3. Diversity of phototrophic microbes in the EAC and Tasman Sea.** Relative
 255 abundance of pico-eukaryote OTUs (97% nucleotide identity) based on the chloroplast 16S
 256 rRNA gene (Decelle et al. 2015). Dominant taxa are labelled at the Family level.

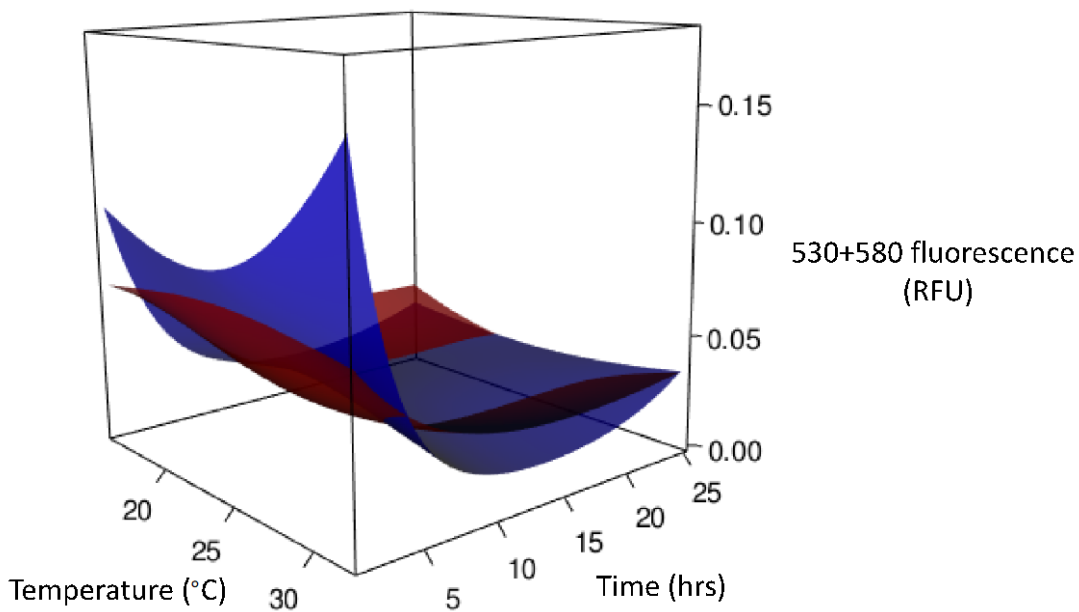
257

258

259



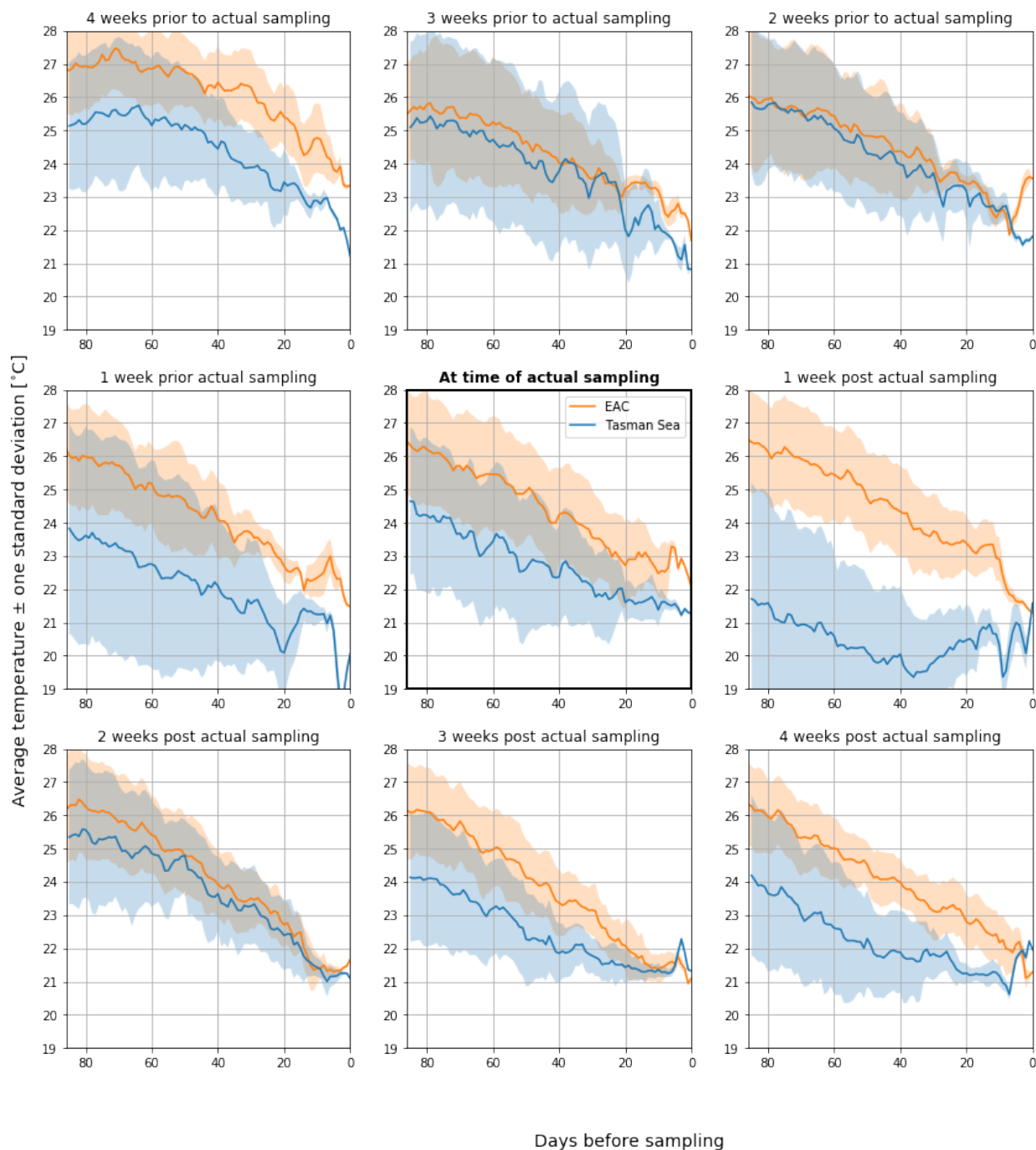
260



261

262 **Fig. S4. Pico-eukaryote response to temperature excursion.** A: Change in the number of ROS
 263 negative (healthy) and ROS positive cells (stressed) in the EAC (A) and Tasman Sea (B)
 264 picoeukaryote populations over the 25 h assay at different temperatures. (C) Contour plot showing
 265 the relationship between ROS expression (530 + 580 nm fluorescence) across temperature and
 266 time in the EAC (red) and Tasman Sea (blue).

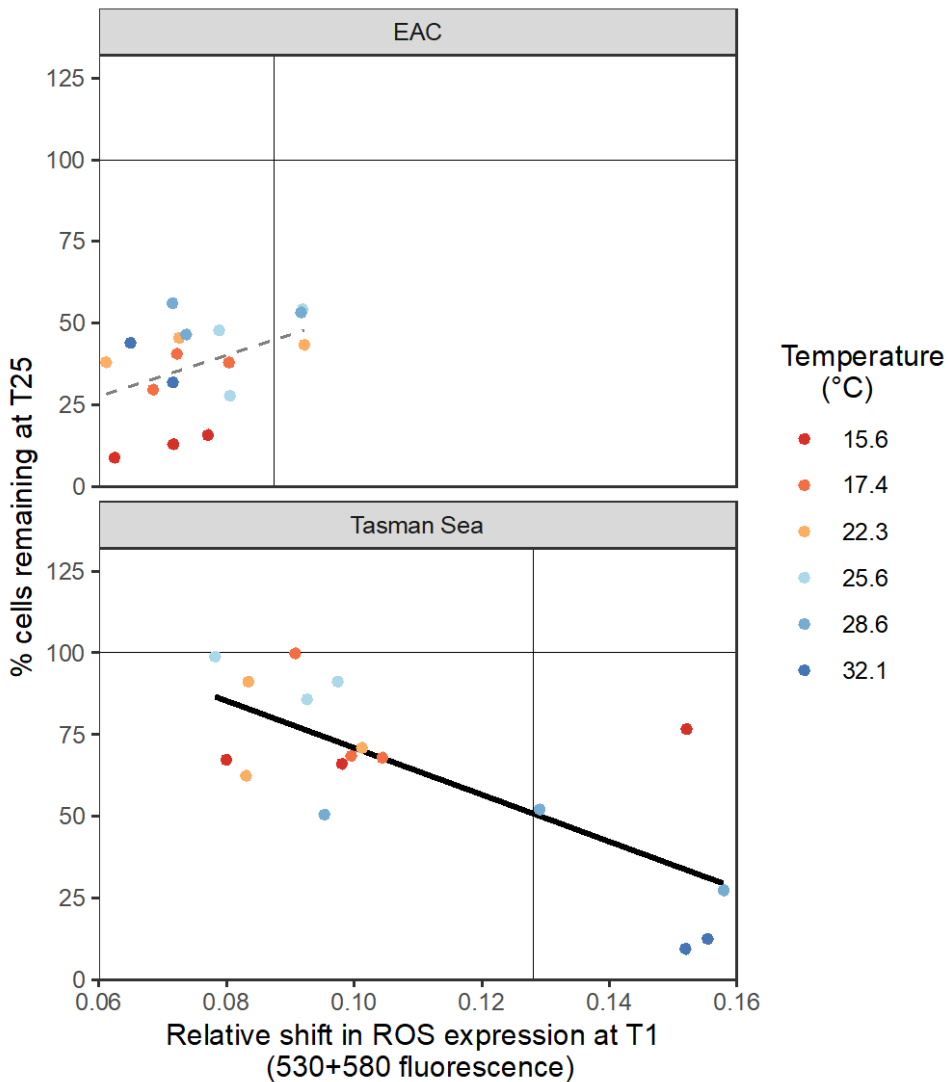
267



269

270 **Fig. S5. Sensitivity analysis of estimated thermal exposure of microbes sampled in this study.**
 271 Central plot shows the estimated thermal trajectories of microbes before they were sampled at
 272 EAC site (orange) on 2015-06-14 (YY-MM-DD) and Tasman Sea site (blue) on 2015-06-13.
 273 Previous and subsequent plots show estimated thermal trajectories from the same sites if they were
 274 sampled 1, 2, 3, or 4 weeks prior or post the actual sampling date.

275



277

278 **Fig. S6. ROS expression is an early indicator of pico-eukaryote mortality.** A large increase in
 279 530 + 580 nm fluorescence of pico-eukaryote cells at T1 relative to T0 is correlated with the lowest
 280 % cells remaining at 25 h. ROS production 1 h after exposure to new temperatures (T1) predicts
 281 longer-term population dynamics (% cells remaining at T25) in pico-eukaryote populations from
 282 the Tasman Sea (solid line, $p < 0.001$, Adjusted $R^2 = 0.528$) but not the EAC (dashed line, $p =$
 283 0.094).

284